PRAMANA
— journal of
physics

Vol. 70, No. 4
April 2008
pp. 697–704

Structural and electrical transport properties of nanosized $La_{0.67}Ca_{0.33}MnO_3$ sample synthesized by a simple low-cost novel route

S KESHRI* and V DAYAL
Department of Applied Physics, Birla Institute of Technology, Mesra, Ranchi 835 215, India
*Corresponding author. E-mail: s_keshri@bitmesra.ac.in; sskeshri@rediffmail.com

MS received 17 May 2007; revised 23 November 2007; accepted 27 November 2007

Abstract. We have synthesized nanosized $La_{0.67}Ca_{0.33}MnO_3$ by a simple low-cost novel synthesis route without calcination at high temperature. The study of these nanoparticles indicates excellent properties similar to colossal magnetoresistance (CMR) materials sintered at ∼1600°C for 20 h. The resulting particle size is in the range of 50–160 nm as determined by scanning electron microscopy. Resistivity measurement has been carried out down to 12 K. The sample shows metal-to-insulator (M–I) transition at 205 K.

Keywords. Nanosized LCMO; polyvinyl alcohol route; X-ray diffraction; scanning electron microscope.

PACS Nos 71.30.+h; 72.10.Bg

1. Introduction

The discovery of manganese-based perovskite materials, called the colossal magnetoresistive (CMR) materials, has generated a considerable interest because of their various electronic, magnetic and structural properties and potential applications [1–3]. Soon after the discovery and publication of the properties of CMR materials [1], there has been considerable experimental and theoretical interest in perovskite manganese oxides of the type $R_{1-x}A_xMnO_3$, where R and A are rare earth and alkaline-earth elements, respectively. These systems are known to exhibit a number of unusual and interesting electronic properties amongst which, the temperature-dependent insulator–metal transition and the CMR effect are probably the most dramatic one. The parent compound $RMnO_3$ which is an antiferromagnetic, when doped with divalent ions (A), can be driven into a metallic ferromagnetic state due to conversion of proportional number of Mn^{3+} to Mn^{4+} via O^{2-}; the process is known as 'double exchange (DE)' mechanism proposed by Zener [4]. But later study pointed out that DE alone cannot explain all the physics of these types of

compounds. The other important factors governing the magnetic and transport behaviours in manganites are Jahn–Teller distortion and electron–phonon coupling [5].

The bulk polycrystalline samples of perovskite-type lanthanum manganese oxides are usually prepared by the conventional solid state reaction method that needs higher temperature (∼1600°C) and longer sintering time to obtain a homogenous composition and desired structural property [6]. Until now, a large number of methods such as co-precipitation [7], sol–gel [8], hydrothermal [9], micro-emulsion [10], metal-organic thermal decomposition [11], chemical technique [12] by polyvinyl alcohol (PVA) route etc. are used to synthesize fine or ultra-fine particles with desired size and narrow distribution. The physical properties of these samples are usually dependent on their preparation routes [13]. Furthermore, the nanostructured material has been predicted to provide some new features in magnetic properties compared to bulk materials [14,15]. The PVA method is a simple low-cost novel synthesis route to synthesize nanosized lanthanum manganese oxides at relatively low calcination temperature. Sahu *et al* [12] and Battabyal *et al* [12] have followed this technique to synthesize nanosized $La_{0.7}Sr_{0.3}MnO_3$ and $La_{1-x}Ag_xMnO_3$ respectively. In the present paper, we have used this method to grow nanosized $La_{0.67}Ca_{0.33}MnO_3$ (LCMO). Crystal property of the grown composition has been studied using X-ray diffractometer. The morphological and compositional analyses have been studied by scanning electron microscope (SEM) and EDAX analysis respectively. The resistivity of the sample has been measured at cryogenic temperatures.

2. Experimental

Powder sample of $La_{0.67}Ca_{0.33}MnO_3$ has been prepared through thermolysis of an aqueous, polymeric-bond precursor solution starting from La_2O_3 and $CaCO_3$, in appropriate stoichiometric amounts dissolved in dilute nitric acid to obtain stocks of respective metal nitrates and $(CH_3COO)_2Mn{\cdot}4H_2O$ in distilled water. The nitrate stocks and the manganese acetate solution were mixed and heated to about 80°C. Into the hot solution, calculated amounts of polyvinyl alcohol (PVA), triethanol amine (TEA) and sucrose have been added in molar ratio to obtain the final stock solution. The final stock solution was heated at ∼200°C on the hot plate with continuous stirring and was heated up to dryness. On complete evaporation, the precursor solution gave rise to a fully burnt organic mass containing the desired metal ions embedded in its matrix. The carbon-rich mass was crushed to constitute the precursor powders. Subsequent calcinations of the precursors at 800°C for 12 h results in carbon-free, nanosized powder having the desired composition. Pellet prepared from this precursor powder has been heated at 1100°C for more than 24 h and then furnace cooled to room temperature.

The powder X-ray diffraction pattern was recorded at room temperature using Rigaku diffractometer with CuK_α radiation. The morphological analysis of the sample was carried out using QUANTA 200 F scanning electron microscope (SEM). The resistivity of the samples was measured at cryogenic temperatures using four-probe technique.

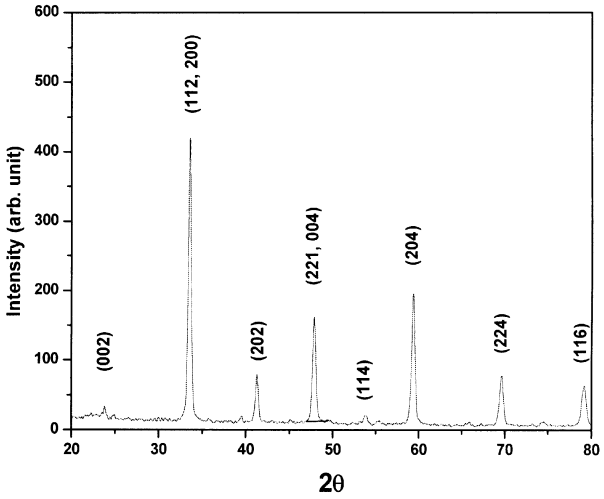

Figure 1. XRD pattern of LCMO sample.

3. Results and discussion

Figure 1 displays the X-ray diffraction patterns of the grown sample completely indexable to a tetragonal unit cell with $a = b = 5.45$ Å and $c = 7.69$ Å. Grain size has been calculated using the Scherrer formula [16]

$$S = K\lambda/\beta\cos\theta, \tag{1}$$

where the constant K depends on the shape of the grain size (=0.89, assuming the circular grain), β=FWHM, λ is the wavelength of the CuK_α radiation and θ is the glancing angle. The grain size of the sample is found to be $\sim$42$\pm$1.18 nm, by considering that the grains are circular in shape. This calculated result is, however, not exactly the same as the value of grain size obtained from the scanning electron micrograph of the sample (see figure 2). According to the micrograph, grain size ranges from 50 nm to 160 nm; some are even bigger. The grain growths of different sizes have perhaps occurred because we have not shivered the composition during its synthesis. The compositional ratio, as calculated from chemical formula and EDAX analysis, are compared in table 1. From this table it is noted that our sample contains all the compositional elements except oxygen, close to the desired values.

Temperature (T) variation of electrical resistivity (ρ) of the synthesized samples is shown in figure 3. The sample exhibits metal–insulator transition at a metal–insulator transition temperature ($T_{\rm MI}$) of 205 K which is slightly lower than the value of $T_{\rm MI}$ = 221.5 K of the same composition synthesized by solid state route [17]; also the resistivity of the present sample is lesser compared to the other for the entire temperature range. The resistivity data in the metallic region, i.e. below $T_{\rm MI}$, could be well-fitted to the empirical relation [18]:

$$\rho = \rho_0 + \rho_1 T^n \tag{2}$$

Table 1. The compositional ratio of $La_{0.67}Ca_{0.33}MnO_3$, calculated from chemical formula and EDAX analysis.

	From chemical formula		From EDAX analysis	
Elements	Wt. %	At. %	Wt. %	At. %
La	61.60	13.40	53.66	21.97
Ca	04.40	06.60	07.67	10.88
Mn	18.20	20.00	27.90	28.88
O	15.90	60.00	10.77	38.27

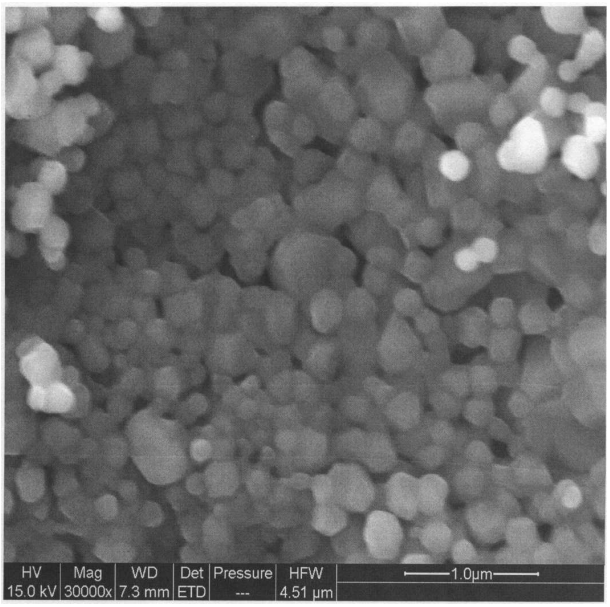

Figure 2. SEM of LCMO sample.

with $n = 2$ to 3. Here ρ_0 and ρ_1 are constants. The typical values of the parameters obtained from the fit of eq. (2) are listed in table 2. The fitted graph is shown by solid line in figure 3 and the fitted parameters are shown in table 2. The value of n has been found to be 2.58±0.003 which indicates a combined effect of scattering of electron–electron, electron–phonon and electron–magnon.

From the thermally activated conduction (TAC) law the resistivity is expressed as

$$\rho = \rho_{\text{oh}} \exp \frac{E_{\text{a}}}{k_{\text{B}}T}, \tag{3}$$

where ρ_{oh} is a constant, k_{B} is the Boltzmann's constant and E_{a} is the activation energy. The best-fitted values of ρ_{oh} and E_{a} are enlisted in table 2.

Table 2. Parameters obtained from the fittings of experimental data using eqs (2)–(4).

	$T < T_{\mathrm{MI}}$					$T > T_{\mathrm{MI}}$				
	Empirical relation $\rho = \rho_0 + \rho_1 T^n$			TAC law $\rho = \rho_{\mathrm{oh}} \exp(E_{\mathrm{a}}/k_{\mathrm{B}}T)$		VRH model $\rho = \rho_{\mathrm{oh}} \exp(T_{\mathrm{o}}/T)$				
Technique of growth	ρ_0 (Ω-cm)	ρ_1 (Ω-cm)	n	E_{a} (meV)	ρ_{oh} (Ω-cm)	ρ_{oh} (Ω-cm)	$T_{\mathrm{o}} \times 10^3$ (K)	$N(E_{\mathrm{F}}) \times 10^{23}$ $(\mathrm{eV})^{-1}\ \mathrm{m}^{-1}$	$R_{\mathrm{hop}}(T)$ (Å)	$E_{\mathrm{hop}}(T)$ (meV)
PVA	2.25±0.0057	0.02×10^{-3} $\pm3.10\times10^{-7}$	2.58±0.003	126.58	0.0177	0.0177	5.87	5.95	3.15	13.6
Solid state	107.33±1.62	4.50±1.01	2.05±0.04	126.69±5.03	0.41±0.06	0.41±0.06	7.08±0.17	46.6	3.30	14.25

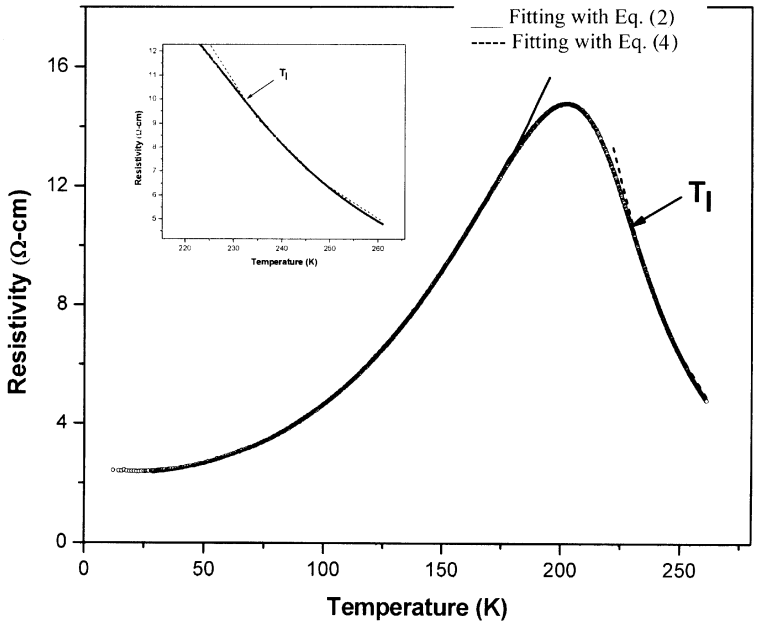

Figure 3. Resistance vs. temperature curve with its theoretical fittings by VRH model.

We have fitted the $\rho(T)$ data for $T > T_{\mathrm{MI}}$ to the variable range hopping (VRH) model [18] also. The original expression due to Mott is given by

$$\rho = \rho_{\mathrm{oh}} \exp\left(\frac{T_{\mathrm{o}}}{T}\right)^{1/4}, \tag{4}$$

where

$$T_{\mathrm{o}} = \frac{18}{k_{\mathrm{B}} N(E_{\mathrm{F}}) a^3} \tag{5}$$

and ρ_{oh} is a constant. Here $N(E_{\mathrm{F}})$ is the density of state in the vicinity of Fermi energy and a is the localization length. The expression (5) describes hopping transport in a system where the carriers are localized by random potential fluctuations and the preferred hopping is between sites lying within a certain range of energies. The mean hopping distance $R_{\mathrm{hop}}(T)$ and mean hopping energy $E_{\mathrm{hop}}(T)$ at temperature T (ref. [18]) are given as follows:

$$R_{\mathrm{hop}}(T) = \frac{3}{8} a \left(\frac{T_{\mathrm{o}}}{T}\right)^{1/4} \tag{6}$$

$$E_{\mathrm{hop}}(T) = \frac{1}{4} k_{\mathrm{B}} T^{3/4} T_{\mathrm{o}}^{1/4}. \tag{7}$$

The best-fitted values of the parameters obtained from the fit of LCMO are given in table 2 and the fitted curve is shown as dotted line in figure 3. We have estimated the values of mean hopping distance ($R_{\rm hop}$), mean hopping energy ($E_{\rm hop}$) at 300 K, and the density of states, $N(E_{\rm F})$, using the best-fitted value of $T_{\rm o}$ and enlisted in table 2. In the above calculation we have assumed the localization length a to be 3.9 a.u. as considered by Okimoto *et al* [19]. Similar estimated parameters for the same sample synthesized by solid state method [17] are also enlisted in table 2 for comparison.

4. Conclusion

Chemical synthesis route is technically simple and economical for large-scale production of nanocrystalline LCMO materials. The electrical property of the compound is found similar to that of samples prepared by the conventional high temperature solid state reaction method. The resistivity data in the metallic region, i.e. below $T_{\rm MI}$ could be well-fitted to the empirical relation (eq. (2)) whereas the same for $T > T_{\rm MI}$ temperature range has been analysed using TAC law (eq. (3)). The experimental data of resistivity for $T > T_{\rm MI}$ temperature range have also been fitted using VRH models and the fitting has been found reasonably well (figure 3).

References

[1] P Schiffer, A P Ramirez, W Bao and S-W Cheong, *Phys. Rev. Lett.* **75**, 3336 (1995)
[2] G T Tan, S Y Dai, P Duan, Y L Zhou, H B Hu and Z H Chen, *J. Appl. Phys.* **93**, 5480 (2003)
[3] S Roy and N Ali, *J. Appl. Phys.* **89**, 7425 (2001)
[4] C Zener, *Phys. Rev.* **82**, 403 (1951)
[5] A J Millis, *Nature (London)* **392**, 147 (1998)
[6] For example, M S Sahasrabudhe, S I Patil, S K Date, K P Adhi, S D Kulkarni, P A Joy and R N Bathe, *Solid State Commun.* **137**, 595 (2006)
V Dayal and S Keshri, *Solid State Commun.* **142**, 63 (2007)
[7] For example, G R Fox, E Breval and R E Newnham, *J. Mater. Sci.* **26**, 2556 (1991)
[8] For example, J Gutiérrez, V Siruguri, J M Barandiarán, A Peña, L Lezama and T Rojo, *Physica* **B372**, 173 (2006)
[9] For example, H Cheng, J Ma, Z Zhao and L Qi, *J. Mater. Sci. Lett.* **15**, 1245 (1996)
[10] J Fang, J Wang, S C Nag, C H Chew and L M Gan, *J. Mater. Sci.* **34**, 1943 (1999)
[11] Y H Huang, Z G Xu, C H Yan, Z M Wang, T Zhu, C S Liao, S Gao and G X Xu, *Solid State Commun.* **114**, 43 (2000)
[12] For example, D R Sahu, B K Roul, P Pramanik and Jow-Lay Huang, *Physica* **B369**, 209 (2005)
M Battabyal and T K Dey, *Solid State Commun.* **131**, 337 (2004)
[13] C N R Rao, R Mahesh, A K Raychaudhuri and R Mahendiran, *J. Phys. Chem. Solids* **59**, 487 (1998)
[14] T A Yamamoto, M Tanaka, Y Misaka, T Nakagawa, K Niihara and T Numazawa, *Scripta Mater.* **46**, 89 (2002)
[15] G Wang, Z D Wang and L D Zhang, *Mater. Sci. Eng.* **B116**, 183 (2005)
[16] A Taylor, *X-ray metallography* (Wiley, New York, 1961)

[17] S Keshri, V Dayal and L Joshi, *Phase Transitions* **81**, 17 (2008)
[18] For example, R Ang, W J Lu, R L Zhang, B C Zhao, X B Zhu, W H Song and Y P Sun, *Phys. Rev.* **B72**, 184417 (2005)
G J Snyder, R Hiskes, S DiCarolis, M R Beasley and T H Geballe, *Phys. Rev.* **B53**, 14434 (1996)
[19] Y Okimoto, T Katsufuji, T Ishikawa, A Urushibara, T Arima and Y Tokura, *Phys. Rev. Lett.* **75,** 109 (1995)